Available online at www.sciencedirect.com
ScienceDirect
Acta Materialia 55 (2007) 5269–5279
Acta MATERIALIA
www.elsevier.com/locate/actamat

The role of defects in the design of space elevator cable: From nanotube to megatube

Nicola M. Pugno *

Department of Structural Engineering and Geotechnics, Politecnico di Torino, Corso Duca degli Abruzzi 24, 10129 Torino, Italy

Received 5 April 2007; received in revised form 29 May 2007; accepted 29 May 2007
Available online 25 July 2007

Abstract

Researchers are claiming that the feasibility of space elevator cable is now realistic, thanks to carbon nanotube technology, proposing its realization within a decade. However, the current view of basing the design of the megacable on the theoretical strength of a single carbon nanotube is naïve, as has recently been emphasized. In this paper the role of thermodynamically unavoidable atomistic defects with different size and shape is quantified on brittle fracture, fatigue and elasticity, for nanotubes and nanotube bundles. Nonasymptotic regimes, elastic plasticity, rough cracks, finite domains and size effects are also discussed. The results are compared with atomistic simulations and nanotensile tests of carbon nanotubes. Key simple formulas for the design of a flaw-tolerant space elevator megacable are reported, suggesting that it would need a taper ratio (for uniform stress) of about two orders of magnitude larger than currently proposed.

Keywords: Fracture; Scaling; Nanocomposite; Stress rupture; Toughness

1. Introduction

A space elevator basically consists of a cable attached to the Earth's surface for carrying payloads into space [1]. If the cable is long enough, i.e. around 150 Mm (a value that can be reduced by a counterweight), the centrifugal forces exceed the gravity of the cable that will work under tension [2]. The elevator would stay fixed geosynchronously; once sent far enough, climbers would be accelerated by the Earth's rotational energy. A space elevator would revolutionize the methodology for carrying payloads into space at low cost, but its design is very challenging. The most critical component in the space elevator design is undoubtedly the cable [3], which requires a material with very high strength and low density.

If we consider a cable with constant cross-section and a vanishing tension at the planet surface, the maximum stress–density ratio for the Earth, reached at the geosynchronous orbit, is 63 GPa/(1300 kg m^{-3}), corresponding to 63 GPa if low carbon density is assumed for the cable. It is only recently, after the discovery of carbon nanotubes [4], that such large failure stresses have been measured experimentally, during tensile tests on ropes composed of single-walled [5] or multiwalled [6–8] carbon nanotubes, both of which were expected to have an ideal strength of ~100 GPa. Note that for steel (density 7900 kg m^{-3}, maximum strength 5 GPa) the maximum stress expected in the cable would be 383 GPa, whereas for Kevlar (density 1440 kg m^{-3}, strength 3.6 GPa) it would be 70 GPa, both much higher than their respective strengths [3].

However, an optimized cable design must consider a uniform tensile stress profile rather than a constant cross-sectional area [2]. Accordingly, the cable could be built from any material simply by using a sufficiently large taper ratio, i.e., the ratio of the maximum (at the geosynchronous orbit) to the minimum (at the Earth's surface) cross-sectional area. For example, for steel and Kevlar huge and unrealistic taper ratios of 10^{33} and 2.6×10^{8}, respectively, would be required, whereas for carbon

* Tel.: +39 011 564 4902; fax: +39 011 564 4899.
E-mail address: nicola.pugno@polito.it

1359-6454/$30.00
doi:10.1016/j.actamat.2007.05.052

nanotubes the taper ratio would theoretically be only 1.9 [9]. Thus, the feasibility of the space elevator seems to become currently plausible [9,10] thanks to the discovery of carbon nanotubes. The cable would represent the largest engineering structure, hierarchically designed from the nanoscale (single nanotube with length of the order of a hundred nanometers) to the megascale (space elevator cable with length of the order of a hundred megameters). But basing the design of the megacable on the theoretical strength of a single carbon nanotube, as in the current view, is in the author's opinion naïve [3] (see also the related news@nature, 22 May 2006, "The space elevator: going down?" by J. Palmer).

In this paper the asymptotic analysis on the role of defects for the megacable strength, based on new theoretical deterministic and statistical approaches of quantized fracture mechanics proposed by the author [11–14], is extended to nonasymptotic regimes, elastic plasticity, rough cracks and finite domains. The role of thermodynamically unavoidable atomistic defects with different size and shape is quantified on brittle fracture, fatigue and elasticity, for nanotubes and nanotube bundles. The results are compared with atomistic simulations and nanotensile tests of carbon nanotubes. Key simple formulas for the design of a flaw-tolerant space elevator megacable are reported, suggesting that it would need a taper ratio (for uniform stress) of about two orders of magnitude larger than currently proposed.

The paper is organized in ten short sections, as follows. After this introduction, we begin by demonstrating that defects are thermodynamically unavoidable, evaluating their vacancy fraction in Section 2. In Section 3 the strength reduction of a single nanotube and of a nanotube bundle containing defects with given size and shape is calculated; the taper ratio for a flaw-tolerant space elevator cable is accordingly derived. In Section 4 elastic–plastic (or hyperelastic) materials, rough cracks and finite domains are discussed. In Section 5 the fatigue lifetime is evaluated for a single nanotube and for a nanotube bundle. In Section 6 the related Young's modulus degradations are quantified. In Sections 7 and 8 the results on strength and elasticity are compared with atomistic simulations and tensile tests of carbon nanotubes. In Section 9 size effects are discussed. The last section presents some concluding remarks.

2. Thermodynamically unavoidable defects

Defects are statistically expected, especially in such huge a bundle. In particular, the entropy increment S due to the formation of n monovacancies in a nanotube (bundle or crystal) composed of N atoms is, according to Boltzmann, given by $S = k_B \ln N!/[(N-n)!n!]$ (k_B is Boltzmann's constant); thus, the free-energy variation is $F = nE_1 - TS$, where T is the absolute temperature and E_1 is the energy required to extract one atom from the nanotube. At the thermal equilibrium, $\partial F/\partial n = 0$, and consequently the vacancy fraction is estimated (for constant volume, neglecting the variation of the strain energy and assuming $n \ll N$) as [15]

$$v = \frac{n}{N} \approx \mathrm{e}^{-\frac{E_1}{k_B T}} \tag{1}$$

For the megacable, having a carbon weigh of ~5000 Kg, $N \approx 5 \times 10^6/12 \cdot N_A \approx 2.5 \times 10^{29}$ (N_A is Avogadro's number) and $E_1 \approx 7$ eV; considering the temperature at which the carbon is assembled, typically in the range between 2000 and 4000 K [16], gives a huge number of equilibrium defects, in the range from 0.6×10^{12} to 3.9×10^{20}, in agreement with recent discussions [16] and observations [17]. Thus, defects are unavoidable, even if small vacancy fractions ($v \approx 2.4 \times 10^{-18}$ to 1.6×10^{-9}) can be achieved. Note that in Ref. [16] it is stated that there is no carbon tube which can match the strength of iron beyond a scale of 2 mm; even if this claim is questionable, it is clearly in agreement with our doubts.

3. Brittle fracture

By considering quantized fracture mechanics (QFM; [11–14]), the failure stress σ_N for a nanotube having atomic size q (the "fracture quantum") and containing an elliptical hole of half-axes a, perpendicular to the applied load (or nanotube axis), and b can be determined, including in the asymptotic solution [12] the contribution of the far-field stress. We accordingly derive

$$\frac{\sigma_N(a,b)}{\sigma_N^{(\mathrm{theo})}} = \sqrt{\frac{1 + 2a/q(1 + 2a/b)^{-2}}{1 + 2a/q}}, \quad \sigma_N^{(\mathrm{theo})} = \frac{K_{IC}}{\sqrt{q\pi/2}} \tag{2}$$

where $\sigma_N^{(\mathrm{theo})}$ is the theoretical (defect-free) nanotube strength (~100 GPa, see Table 1) and K_{IC} is the material fracture toughness. The self-interaction between the tips has been here neglected (i.e. $a \ll \pi R$, with R nanotube radius) and would further reduce the failure stress. For atomistic defects (having a characteristic length of a few ångströms) in nanotubes (having a characteristic diameter of several nanometers) this hypothesis is fully verified. However, QFM can also easily treat the self-tip interaction starting from the corresponding value of the stress-intensity factor (reported in the related handbooks). The validity of QFM has been recently confirmed by atomistic simulations [3,12,13,18], but also at larger size-scales [12,13,19] and for fatigue crack growth [14,20,21].

With regard to the defect shape, for a sharp crack perpendicular to the applied load, $a/q = \mathrm{const}$ and $b/q \to 0$, so $\sigma_N \approx \sigma_N^{(\mathrm{theo})}/\sqrt{1 + 2a/q}$, and for $a/q \gg 1$, i.e. large cracks, $\sigma_N \approx K_{IC}/\sqrt{\pi a}$, in agreement with linear elastic fracture mechanics (LEFM). Note that LEFM (i) can only treat sharp cracks and (ii) unreasonably predicts an infinite defect-free strength. On the other hand, for a crack parallel to the applied load, $b/q = \mathrm{const}$ and $a/q \to 0$, and so $\sigma_N = \sigma_N^{(\mathrm{theo})}$, as it should be. In addition, with regard to the defect size, for self-similar and small holes, $a/b = \mathrm{const}$

Table 1
Atomistic simulations [29–32] vs. QFM [11–14] strength predictions, for nanocracks of size n or nanoholes of size m

Nanotube type	Nanocrack (n) and nanohole (m) sizes	Strength (GPa) by QM (MTB-G2), MM (PM3; M) and QM/MM atomistic or QFM calculations
[5,5]	Defect-free	105 (MTB-G2); 135 (PM3)
[5,5]	$n=1$ (sym. + H)	85 (MTB-G2), 79 (QFM); 106 (PM3), 101 (QFM)
[5,5]	$n=1$ (Asym. + H)	71 (MTB-G2), 79 (QFM); 99 (PM3), 101 (QFM)
[5,5]	$n=1$ (Asym.)	70 (MTB-G2), 79 (QFM); 100 (PM3), 101 (QFM)
[5,5]	$n=2$ (Sym.)	71 (MTB-G2), 63 (QFM); 105 (PM3), 81 (QFM)
[5,5]	$n=2$ (Asym.)	73 (MTB-G2), 63 (QFM); 111 (PM3), 81 (QFM)
[5,5]	$m=1$ (+H)	70 (MTB-G2), 68 for long tube, 79 (QFM); 101 (PM3), 101 (QFM)
[5,5]	$m=2$ (+H)	53 (MTB-G2), 50 for long tube, 67 (QFM); 78 (PM3), 86 (QFM)
[10,10]	Defect-free	88 (MTB-G2); 124 (PM3)
[10,10]	$n=1$ (sym. + H)	65 (MTB-G2), 66 (QFM)
[10,10]	$n=1$ (Asym. + H)	68 (MTB-G2), 66 (QFM)
[10,10]	$n=1$ (Sym.)	65 (MTB-G2), 66 (QFM); 101 (PM3), 93 (QFM)
[10,10]	$n=2$ (Sym.)	64 (MTB-G2), 53 (QFM); 107 (PM3), 74 (QFM)
[10,10]	$n=2$ (Asym.)	65 (MTB-G2), 53 (QFM); 92 (PM3), 74 (QFM)
[10,10]	$m=1$ (+H)	56 (MTB-G2), 52 for long tube, 66 (QFM); 89 (PM3), 93 (QFM)
[10,10]	$m=2$ (+H)	42 (MTB-G2), 36 for long tube, 56 (QFM); 67 (PM3), 79 (QFM)
[50,0]	Defect-free	89 (MTB-G2)
[50,0]	$m=1$ (+H)	58 (MTB-G2); 67 (QFM)
[50,0]	$m=2$ (+H)	46 (MTB-G2); 57 (QFM)
[50,0]	$m=3$ (+H)	40 (MTB-G2); 44 (QFM)
[50,0]	$m=4$ (+H)	36 (MTB-G2); 41 (QFM)
[50,0]	$m=5$ (+H)	33 (MTB-G2); 39 (QFM)
[50,0]	$m=6$ (+H)	31 (MTB-G2); 37 (QFM)
[100,0]	Defect-free	89 (MTB-G2)
[100,0]	$m=1$ (+H)	58 (MTB-G2); 67 (QFM)
[100,0]	$m=2$ (+H)	47 (MTB-G2); 57 (QFM)
[100,0]	$m=3$ (+H)	42 (MTB-G2); 44 (QFM)
[100,0]	$m=4$ (+H)	39 (MTB-G2); 41 (QFM)
[100,0]	$m=5$ (+H)	37 (MTB-G2); 39 (QFM)
[100,0]	$m=6$ (+H)	35 (MTB-G2); 37 (QFM)
[29,29]	Defect-free	101 (MTB-G2)
[29,29]	$m=1$ (+H)	77 (MTB-G2); 76 (QFM)
[29,29]	$m=2$ (+H)	62 (MTB-G2); 65 (QFM)
[29,29]	$m=3$ (+H)	54 (MTB-G2); 50 (QFM)
[29,29]	$m=4$ (+H)	48 (MTB-G2); 46 (QFM)
[29,29]	$m=5$ (+H)	45 (MTB-G2); 44 (QFM)
[29,29]	$m=6$ (+H)	42 (MTB-G2); 42 (QFM)
[47,5]	Defect-free	89 (MTB-G2)
[47,5]	$m=1$ (+H)	57 (MTB-G2); 67 (QFM)
[44,10]	Defect-free	89 (MTB-G2)
[44,10]	$m=1$ (+H)	58 (MTB-G2); 67 (QFM)
[40,16]	Defect-free	92 (MTB-G2)
[40,16]	$m=1$ (+H)	59 (MTB-G2); 69 (QFM)
[36,21]	Defect-free	96 (MTB-G2)
[36,21]	$m=1$ (+H)	63 (MTB-G2); 72 (QFM)
[33,24]	Defect-free	99 (MTB-G2)
[33,24]	$m=1$ (+H)	67 (MTB-G2); 74 (QFM)
[80,0]	Defect-free	93 (M)
[80,0]	$n=2$	64 (M); 56 (QFM)
[80,0]	$n=4$	50 (M); 43 (QFM)
[80,0]	$n=6$	42 (M); 35 (QFM)
[80,0]	$n=8$	37 (M); 32 (QFM)
[40,0] (nested by a [32,0])	Defect-free	99 (M)
[40,0] (nested by a [32,0])	$n=2$	73 (M); 69 (QFM + vdW interaction ~10 GPa)

(*continued on next page*)

Table 1 (*continued*)

Nanotube type	Nanocrack (n) and nanohole (m) sizes	Strength (GPa) by QM (MTB-G2), MM (PM3; M) and QM/MM atomistic or QFM calculations
[40,0] (nested by a [32,0])	$n=4$	57 (M); 56 (QFM + vdW interaction ~10 GPa)
[40,0] (nested by a [32,0])	$n=6$	50 (M); 48 (QFM + vdW interaction ~10 GPa)
[40,0] (nested by a [32,0])	$n=8$	44 (M); 44 (QFM + vdW interaction ~10 GPa)
[100,0]	Defect-free	89 (MTB-G2)
[100,0]	$n=4$	50 (M); 41 (QFM)
[10,0]	Defect-free	124 (QM); 88 (MM);
[10,0]	$n=1$	101 (QM) 95 (QM/MM) 93 (QFM); 65 (MM) 66 (QFM)

The QFM predictions are here obtained simply considering in Eq. (2) $2a/q=n$, $2b/q=1$ for cracks of size n or $a/q=b/q=(2m-1)/\sqrt{3}$ for holes of size m (differently from the asymptotic treatment reported in [3]). Quantum mechanics (QM) semi-empirical calculations (PM3 method), molecular mechanics (MM) calculations (modified Tersoff–Brenner potential of second generation (MTB-G2), modified Morse potential (M)) and coupled QM/MM calculations. The symbol (+H) means that the defect was saturated with hydrogen. Symmetric and asymmetric bond reconstructions were also considered; the tubes are "short" if not otherwise specified. We have roughly ignored in the QFM predictions the difference between symmetric and asymmetric bond reconstruction, hydrogen saturation and length effect (for shorter tubes an increment in the strength is always observed, as an intrinsic size effect), noting that the main differences in the atomistic simulations are attributable to the potential used. For nested nanotubes a strength increment of ~10 GPa is here assumed to roughly take into account the van der Walls (vdW) interaction between the walls.

and $a/q\to 0$ and coherently $\sigma_N=\sigma_N^{(theo)}$; furthermore, for self-similar and large holes, $a/b=$ const and $a/q\to\infty$ and we deduce $\sigma_N\approx\sigma_N^{(theo)}/(1+2a/b)$, in agreement with the stress concentration posed by elasticity; but elasticity (coupled with a maximum stress criterion) unreasonably predicts a strength (iii) independent of the hole size and (iv) tending to zero for cracks. Note the extreme consistency of Eq. (2), that removing all the limitations (i)–(iv) represents the first law capable of describing in a unified manner all the size and shape effects for the elliptical holes, including cracks as a limiting case. In other words, Eq. (2) shows that the two classical strength predictions based on stress intensifications (LEFM) or stress concentrations (Elasticity) are only reasonable for "large" defects; Eq. (2) unifies their results and extends its validity to "small" defects ("large" and "small" are here with respect to the fracture quantum). Eq. (2) shows that even a small defect can dramatically reduce the mechanical strength.

An upper bound for the cable strength can be derived assuming the simultaneous failure of all the defective nanotubes present in the bundle. Accordingly, imposing the critical force equilibrium (mean-field approach) for a cable composed by nanotubes in numerical fractions f_{ab} containing holes of half-axes a and b, we find the cable strength σ_C (ideal if $\sigma_C^{(theo)}$) in the following form:

$$\frac{\sigma_C}{\sigma_C^{(theo)}}=\sum_{a,b}f_{ab}\frac{\sigma_N(a,b)}{\sigma_N^{(theo)}} \tag{3}$$

The summation is extended to all the different holes; the numerical fraction f_{00} of nanotubes is defect-free and $\sum_{a,b}f_{ab}=1$. If all the defective nanotubes in the bundle contain identical holes, then $f_{ab}=f=1-f_{00}$, and the following simple relation between the strength reductions holds: $1-\sigma_C/\sigma_C^{(theo)}=f(1-\sigma_N/\sigma_N^{(theo)})$.

Thus, the taper ratio λ needed to have a uniform stress in the cable [2], under the centrifugal and gravitational forces, must be larger than its theoretical value to design a flaw-tolerant megacable. In fact, according to our analysis, we deduce ($\lambda=e^{\text{const}\cdot\rho_C/\sigma_C}\geqslant\lambda^{(theo)}\approx 1.9$ for carbon nanotubes; ρ_C denotes the material density) that

$$\frac{\lambda}{\lambda^{(theo)}}=\lambda^{(theo)\left(\frac{\sigma_C^{(theo)}}{\sigma_C}-1\right)} \tag{4}$$

Eq. (4) shows that a small defect can dramatically increase the taper ratio required for a flaw-tolerant megacable.

4. Elastic plasticity, fractal cracks and finite domains

The previous equations are based on linear elasticity, i.e., on a linear relationship $\sigma\propto\varepsilon$ between stress σ and strain ε. In contrast, let us assume $\sigma\propto\varepsilon^\kappa$, where $\kappa>1$ denotes hyperelasticity and $\kappa<1$ elastic plasticity. The power of the stress singularity will accordingly be modified [22] from the classical value 1/2 to $\alpha=\kappa/(\kappa+1)$. Thus, the problem is mathematically equivalent to that of a re-entrant corner [23], and consequently we predict

$$\frac{\sigma_N(a,b,\alpha)}{\sigma_N^{(theo)}}=\left(\frac{\sigma_N(a,b)}{\sigma_N^{(theo)}}\right)^{2\alpha},\quad \alpha=\frac{\kappa}{\kappa+1} \tag{5}$$

A crack with a self-similar roughness, mathematically described by a fractal with noninteger dimension D ($1<D<2$), would similarly modify the stress singularity, according to [24,25] $\alpha=(2-D)/2$; thus, with Eq. (5), we can also estimate the role of the crack roughness. Both plasticity and roughness reduce the severity of the defect, whereas hyperelasticity enlarges its effect. For example, for a crack composed by n adjacent vacancies, we found that $\sigma_N/\sigma_N^{(theo)}\approx(1+n)^{-\alpha}$.

However, note that among these three effects only elastic plasticity may have a significant role in carbon nanotubes; in spite of this, fractal cracks could play an important role in nanotube bundles as a consequence of their larger size-scale, which would allow the development of a crack

surface roughness. Hyperelasticity is not expected to be relevant in this context.

According to LEFM and assuming the classical hypothesis of self-similarity ($a_{\max} \propto L$) [25], i.e., the largest crack size is proportional to the characteristic structural size L, we expect a size effect on the strength in the form of the power law $\sigma_C \propto L^{-\alpha}$. For linear elastic materials, $\alpha = 1/2$, as classically considered; but for elastic–plastic materials or fractal cracks $0 \leqslant \alpha \leqslant 1/2$ [25].

Eq. (2) does not consider the defect–boundary interaction. The finite width $2W$, can be treated by applying QFM starting from the related expression of the stress-intensity factor (reported in handbooks). However, to have an idea of the defect–boundary interaction, we apply an approximate method [26], deriving the following correction: $\sigma_N(a,b,W) \approx C(W)\sigma_N(a,b)$, $C(W) \approx (1-a/W)/\left(\sigma_N(a,b)|_{q\to W-a}/\sigma_N^{(\text{theo})}\right)$. (Note that such a correction is valid also for $W \approx a$, whereas for $W \gg a$, it becomes $C(W \gg a) \approx 1 - a/W$.) Similarly, the role of the defect orientation β could be treated by QFM considering the related stress-intensity factor; roughly, one could use the self-consistent approximation $\sigma_N(a,b,\beta) \approx \sigma_N(a,b)\cos^2\beta + \sigma_N(b,a)\sin^2\beta$.

5. Fatigue fracture

The space elevator cable will be cyclically loaded, e.g., by the climbers carrying the payloads, thus fatigue could play a role in its design. By integrating the quantized Paris law, i.e., an extension of the classical Paris law recently proposed especially for nanostructure or nanomaterial applications [14,20,21], we derive the following number of cycles to failure (or lifetime):

$$\frac{C_N(a)}{C_N^{(\text{theo})}} = \frac{(1+q/W)^{1-m/2} - (a/W+q/W)^{1-m/2}}{(1+q/W)^{1-m/2} - (q/W)^{1-m/2}}, \quad m \neq 2 \tag{6a}$$

$$\frac{C_N(a)}{C_N^{(\text{theo})}} = \frac{\ln\{(1+q/W)/(a/W+q/W)\}}{\ln\{(1+q/W)/(q/W)\}}, \quad m = 2 \tag{6b}$$

where $m > 0$ is the material Paris exponent. Note that, according to Wöhler, $C_N^{(\text{theo})} = K\Delta\sigma^{-k}$, where K and k are material constants and $\Delta\sigma$ is the amplitude of the stress range during the oscillations. Even if fatigue experiments in nanotubes are still to be performed, their behaviour is expected to be intermediate between those of Wöhler and Paris, as displayed by all the known materials, and the quantized Paris law basically represents their asymptotic matching (as quantized fracture mechanics basically represents the asymptotic matching between the strength and toughness approaches).

Only defects remaining self-similar during fatigue growth have to be considered, so only a crack (of half-length a) is of interest in this context. By means of Eq. (6) the time to failure reduction can be estimated, similarly to the brittle fracture treated by Eq. (2). For a bundle, considering a mean-field approach (similarly to Eq. (3)) yields

$$\frac{C_C}{C_C^{(\text{theo})}} = \sum_a f_a \frac{C_N(a)}{C_N^{(\text{theo})}} \tag{7}$$

Better predictions could be derived integrating the quantized Paris law for a finite width strip. However, we note that the role of the finite width is already included in Eq. (6), even if these are rigorously valid in the limit of W tending to infinity.

6. Elasticity

Consider a nanotube of lateral surface A under tension and containing a transversal crack of half-length a. Interpreting the incremental compliance, due to the presence of the crack, as a Young's modulus (here denoted by E) degradation we find $\frac{E(a)}{E^{(\text{theo})}} = 1 - 2\pi\frac{a^2}{A}$ [27]. Thus, recursively, considering Q cracks (in the megacable 10^{12}–10^{20} defects are expected; see Section 2) having sizes a_i or, equivalently, M different cracks with multiplicity $Q_i (Q = \sum_{i=1}^{M} Q_i)$, noting that $n_i = \frac{2a_i}{q}$ represents the number of adjacent vacancies in a crack of half-length a_i, with q atomic size, and $v_i = \frac{Q_i n_i}{A/q^2}$ its related numerical (or volumetric) vacancy fraction, we find [27]

$$\frac{E}{E^{(\text{theo})}} = \prod_{i=1}^{Q} \frac{E(a_i)}{E^{(\text{theo})}} \approx 1 - \xi \sum_{i=1}^{M} v_i n_i \tag{8}$$

with $\xi \geqslant \pi/2$, where the equality holds for isolated cracks. Eq. (8) can be applied to nanotubes or nanotube bundles containing defects in volumetric percentages v_i.

Forcing the interpretation of our formalism, we note that $n_i = 1$ would describe a single vacancy, i.e., a small hole. Thus, as a first approximation, different defect geometries, from cracks to circular holes, e.g., elliptical holes, could in principle be treated by Eq. (8); we have to interpret n_i as the ratio between the transversal and longitudinal (parallel to the load) defect sizes ($n_i = a_i/b_i$). Introducing the ith defect eccentricity e_i as the ratio between the lengths of the longer and shorter axes, as a first approximation $n_i(\beta_i) \approx e_i\cos^2\beta_i + 1/e_i\sin^2\beta_i$, where β_i is the defect orientation. For a single defect typology $\frac{E}{E^{(\text{theo})}} \approx 1 - \xi v n$, in contrast to the common assumption $\frac{E}{E^{(\text{theo})}} \approx 1 - v$, rigorously valid only for the cable density, for which $\frac{\rho_C}{\rho_C^{(\text{theo})}} \equiv 1 - v$. Note that the failure strain for a defective nanotube or nanotube bundle can also be predicted, by $\varepsilon_{N,C}/\varepsilon_{N,C}^{(\text{theo})} = (\sigma_{N,C}/\sigma_{N,C}^{(\text{theo})})/(E/E^{(\text{theo})})$.

In contrast to what happens for the strength, large defectiveness is required to have a considerable elastic degradation, even if we have shown that sharp transversal defects could have a role. For example, space elevator cables that are too soft would become dynamically unstable [28].

7. Atomistic simulations

Let us study the influence of nanocracks and circular nanoholes on the strength. We assume that n adjacent

atomic vacancies perpendicular to the load correspond to a blunt nanocrack of length $2a \approx nq$ and thickness $2b \approx q$ (or $2a \approx nq$ with a tip radius of $b^2/a \approx q/2$). Similarly, nanoholes of size m can be considered: the index $m = 1$ corresponds to the removal of an entire hexagonal ring, $m = 2$ to the additional removal of the six hexagons around the former one (i.e., the adjacent perimeter of 18 atoms), $m = 3$ to the additional removal of the neighbouring 12 hexagonal rings (next adjacent perimeter), and so on (thus $a = b \approx q(2m-1)/\sqrt{3}$). Quantum mechanics (QM), semiempirical (PM3 method), molecular mechanics (MM; with a modified Tersoff–Brenner potential of second generation (MTB-G2) or a modified Morse potential (M)) and coupled QM/MM calculations [29–32] are reported and extensively compared in Table 1 with the QFM nonasymptotic predictions of Eq. (2) (differently from the asymptotic comparison reported in Refs. [3,12]). The comparison shows a relevant agreement, confirming and demonstrating that just a few vacancies can dramatically reduce the strength of a single nanotube, or of a nanotube bundle as described by Eq. (3) that predicts for $f \approx 1$, $\sigma_C/\sigma_C^{(theo)} \approx \sigma_N/\sigma_N^{(theo)}$. Assuming large holes ($m \to \infty$) and applying QFM to a defective bundle ($f \approx 1$), we predict $1 - \sigma_C/\sigma_C^{(theo)} \approx 1 - \sigma_N/\sigma_N^{(theo)} \approx 67\%$; but nanocracks surely would be even more critical, especially if interacting with each other or with the boundary. Thus, the expectation for the megacable of a strength larger than ~33 GPa is unrealistic.

Note that an elastic ($\kappa \approx 1$) nearly perfectly plastic ($\kappa \approx 0$) behaviour, with a flow stress at ~30–35 GPa for strains larger than ~3–5%, has been recently observed in tensile tests of carbon nanotubes [8], globally suggesting $\kappa \approx 0.6 - 0.7$; similarly, numerically computed stress–strain curves [33] reveal for an armchair (5,5) carbon nanotube $\kappa \approx 0.8$, whereas for a zigzag (9,0) nanotube $\kappa \approx 0.7$, suggesting that the plastic correction reported in Section 4 could have a role.

Regarding elasticity, we note that Eq. (8) can be viewed as a generalization of the approach proposed in Ref. [34], being able to quantify the constants k_i fitted by atomistic simulations for three different types of defect [27]. In particular, rearranging Eq. (8) and in the limit of three small cracks, we deduce $\frac{E_{th}}{E} \approx 1 + k_1 c_1 + k_2 c_2 + k_3 c_3$, identical to their law (their Eq. (15)), in which $c_i = Q_i/L$ is the linear defect concentration in a nanotube of length L and radius R and $k_i = \frac{\xi c_i n_i^2 q^2}{\pi^2 R}$. These authors consider 1, 2 and 3 atoms missing, with and without reconstructed bonds; for nonreconstructed bonds two alternative defect orientations were investigated for 2 and 3 atoms missing. Even if their defect geometries are much more complex than the nanocracks that we here consider, the comparison between our approach and their atomistic simulations, which does not involve best-fit parameters, shows a good agreement [27].

8. Nanotensile tests

The tremendous defect sensitivity, described by Eq. (2), is confirmed by a statistical analysis based on nanoscale Weibull statistics (NWS, [35]) applied to the nanotensile tests. According to this treatment, the probability of failure P for a nearly defect-free nanotube under a tensile stress σ_N is independent of its volume (or surface), in contrast to classical Weibull statistics [36], namely:

$$P = 1 - \exp -N_N \left(\frac{\sigma_N}{\sigma_0}\right)^w \tag{9}$$

where w is the nanoscale Weibull modulus, σ_0 is the nominal failure stress (i.e., corresponding to a probability of failure of 63%) and $N_N \equiv 1$. In classical Weibull statistics $N_N \equiv V/V_0$ for volume-dominating defects (or $N_N = A/A_0$ for surface-dominating defects), i.e., N_N is the ratio between the volume (or surface) of the structure and a reference volume (or surface). The experimental data [5,6] were treated [35] according to nanoscale and classical Weibull statistics: the coefficients of correlation were found to be much higher for the nanoscale statistics than for the classical statistics (0.93 against 0.67, $w \approx 2.7$ and $\sigma_0 \approx 31$–34 GPa). The data set on MWCNT tensile experiments

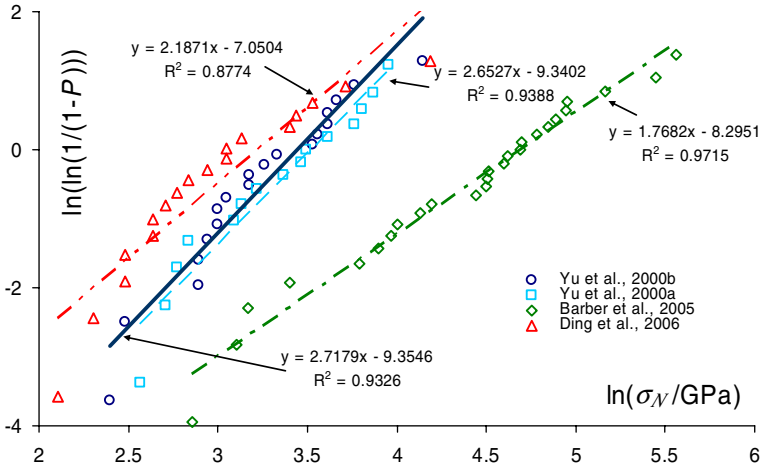

Fig. 1. Nanoscale Weibull statistics [35], straight lines, applied to the new nanotensile experiments on carbon nanotubes [8]. The other three data sets [5–7], already treated with NWS [3,12], are also reported for comparison.

[7] has already been statistically treated [3]. The very large highest measured strengths denote interactions between the external and internal walls, as pointed out by the same authors [7] and recently quantified [14]. Thus, the measured strengths cannot be considered plausible for describing the strength of a SWCNT. Such experiments were best-fitted

Table 2
Experiments [5–8] vs. QFM [11–14] predictions; strength reduction $\sigma_N(a,b)/\sigma_N^{(theo)}$ derived according to Eq. (2)

$\sigma_N/\sigma_N^{(theo)}$	$2b/q$											
$2a/q$	0	1	2	3	4	5	6	7	8	9	10	∞
0	1.00*	1.00*	1.00*	1.00*	1.00*	1.00*	1.00*	1.00*	1.00*	1.00*	1.00*	1.00
1	0.71*	0.75	0.79	0.82	0.85	0.87*	0.88*	0.90	0.91	0.91	0.92	1.00
2	0.58	0.60*	0.64*	0.68	0.71*	0.73	0.76	0.78*	0.79	0.81	0.82	1.00
3	0.50	**0.52**	0.54*	0.58	0.61	0.64*	0.66*	0.68	0.70*	0.72	0.74	1.00
4	**0.45**	0.46	**0.48**	0.51*	0.54*	0.56	0.59	0.61	*0.63*	0.65	0.67	1.00
5	0.41	0.42	0.44*	0.46	**0.48**	0.51*	0.53*	0.55*	0.58	0.59	0.61	1.00
6	0.38	0.38	0.40	0.42	0.44*	0.47	0.49*	0.51*	0.53*	0.55*	0.57	1.00
7	*0.35*	0.36	***0.37***	*0.39*	0.41	***0.43***	**0.45**	0.47	0.49*	0.51*	0.53*	1.00
8	**0.33**	*0.34*	*0.35*	***0.37***	0.38	0.40	0.42	0.44*	0.46	**0.48**	0.49*	1.00
9	**0.32**	**0.32**	**0.33**	*0.34*	0.36	0.38	0.40	0.41	***0.43***	**0.45**	0.46	1.00
10	0.30*	0.30*	0.31	**0.33**	*0.34*	0.36	***0.37***	*0.39*	0.41	0.42	0.44*	1.00
11	**0.29**	**0.29**	0.30*	0.31	**0.32**	*0.34*	*0.35*	***0.37***	*0.39*	0.40	0.42	1.00
12	*0.28*	*0.28*	**0.29**	0.30*	0.31	**0.32**	*0.34*	*0.35*	***0.37***	0.38	0.40	1.00
13	0.27	0.27	*0.28*	**0.29**	0.30*	0.31	**0.32**	*0.34*	*0.35*	0.36	0.38	1.00
14	*0.26*	*0.26*	0.27	0.27	**0.29**	0.30*	0.31	**0.32**	*0.34*	*0.35*	0.36	1.00
15	**0.25**	**0.25**	*0.26*	0.27	0.27	**0.29**	0.30*	0.31	**0.32**	*0.34*	*0.35*	1.00
16	*0.24**	*0.24**	**0.25**	*0.26*	0.27	*0.28*	**0.29**	0.30*	0.31	0.32	**0.33**	1.00
17	*0.24**	*0.24**	*0.24**	**0.25**	*0.26*	0.27	*0.28*	**0.29**	0.30*	0.31	**0.32**	1.00
18	**0.23**	**0.23**	*0.24**	*0.24**	**0.25**	*0.26*	0.27	*0.28*	**0.29**	0.30*	0.31	1.00
19	**0.22***	**0.22***	**0.23**	**0.23**	*0.24**	**0.25**	*0.26*	0.27	*0.28*	**0.29**	0.30*	1.00
20	**0.22***	**0.22***	**0.22***	**0.23**	*0.24**	*0.24**	**0.25**	*0.26*	0.27	*0.28*	**0.29**	1.00
21	*0.21*	*0.21*	**0.22***	**0.22***	**0.23**	*0.24**	**0.25**	**0.25**	*0.26*	0.27	*0.28*	1.00
22	*0.21*	*0.21*	*0.21*	**0.22***	**0.22***	**0.23**	*0.24**	**0.25**	*0.26*	0.27	*0.28*	1.00
23	*0.20*	*0.21*	*0.21*	*0.21*	**0.22***	**0.23**	**0.23**	*0.24**	**0.25**	*0.26*	0.27	1.00
24	*0.20*	*0.20*	*0.20*	*0.21*	*0.21*	**0.22***	**0.23**	*0.24**	*0.24**	**0.25**	*0.26*	1.00
25	*0.20*	*0.20*	*0.20*	*0.20*	*0.21*	**0.22***	**0.22***	**0.23**	*0.24**	**0.25**	*0.26*	1.00
26	*0.19*	*0.19*	*0.20*	*0.20*	*0.20*	*0.21*	**0.22***	**0.22***	**0.23**	*0.24**	**0.25**	1.00
27	*0.19*	*0.19*	*0.19*	*0.20*	*0.20*	*0.21*	*0.21*	**0.22***	**0.23**	*0.24**	*0.24**	1.00
28	*0.19*	*0.19*	*0.19*	*0.19*	*0.20*	*0.20*	*0.21*	**0.22***	**0.22***	**0.23**	*0.24**	1.00
29	*0.18*	*0.18*	*0.19*	*0.19*	*0.19*	*0.20*	*0.20*	*0.21*	**0.22***	**0.23**	**0.23**	1.00
30	*0.18*	*0.18*	*0.18*	*0.19*	*0.19*	*0.19*	*0.20*	*0.21*	*0.21*	**0.22***	**0.23**	1.00
31	*0.18*	*0.18*	*0.18*	*0.18*	*0.19*	*0.19*	*0.20*	*0.20*	*0.21*	**0.22***	**0.22***	1.00
32	**0.17***	**0.17***	*0.18*	*0.18*	*0.18*	*0.19*	*0.19*	*0.20*	*0.21*	*0.21*	**0.22***	1.00
33	**0.17***	**0.17***	**0.17***	*0.18*	*0.18*	*0.19*	*0.19*	*0.20*	*0.20*	*0.21*	*0.21*	1.00
34	**0.17***	**0.17***	**0.17***	**0.17***	*0.18*	*0.18*	*0.19*	*0.19*	*0.20*	*0.20*	*0.21*	1.00
35	**0.17***	**0.17***	**0.17***	**0.17***	**0.17***	*0.18*	*0.18*	*0.19*	*0.19*	*0.20*	*0.21*	1.00
36	**0.16**	**0.16**	**0.17***	**0.17***	**0.17***	*0.18*	*0.18*	*0.19*	*0.19*	*0.20*	*0.20*	1.00
37	**0.16**	**0.16**	**0.16**	**0.17***	**0.17***	**0.17***	*0.18*	*0.18*	*0.19*	*0.19*	*0.20*	1.00
38	**0.16**	**0.16**	**0.16**	**0.16**	**0.17***	**0.17***	*0.18*	*0.18*	*0.19*	*0.19*	*0.20*	1.00
39	**0.16**	**0.16**	**0.16**	**0.16**	**0.17***	**0.17***	**0.17***	*0.18*	*0.18*	*0.19*	*0.19*	1.00
40	**0.16**	**0.16**	**0.16**	**0.16**	**0.16**	**0.17***	**0.17***	*0.18*	*0.18*	*0.19*	*0.19*	1.00
41	**0.15**	**0.15**	**0.16**	**0.16**	**0.16**	**0.16**	**0.17***	**0.17***	*0.18*	*0.18*	*0.19*	1.00
42	**0.15**	**0.15**	**0.15**	**0.16**	**0.16**	**0.16**	**0.17***	**0.17***	*0.18*	*0.18*	*0.19*	1.00
43	**0.15**	**0.15**	**0.15**	**0.15**	**0.16**	**0.16**	**0.16**	**0.17***	**0.17***	*0.18*	*0.18*	1.00
44	**0.15**	**0.15**	**0.15**	**0.15**	**0.16**	**0.16**	**0.16**	**0.17***	**0.17***	*0.18*	*0.18*	1.00
45	**0.15**	**0.15**	**0.15**	**0.15**	**0.15**	**0.16**	**0.16**	**0.16**	**0.17***	**0.17***	*0.18*	1.00
46	**0.15**	**0.15**	**0.15**	**0.15**	**0.15**	**0.15**	**0.16**	**0.16**	**0.17***	**0.17***	*0.18*	1.00
47	0.14	0.14	**0.15**	**0.15**	**0.15**	**0.15**	**0.16**	**0.16**	**0.16**	**0.17***	**0.17***	1.00
48	0.14	0.14	0.14	**0.15**	**0.15**	**0.15**	**0.15**	**0.16**	**0.16**	**0.17***	**0.17***	1.00
49	0.14	0.14	0.14	0.14	**0.15**	**0.15**	**0.15**	**0.16**	**0.16**	**0.16**	**0.17***	1.00
50	0.14	0.14	0.14	0.14	**0.15**	**0.15**	**0.15**	**0.15**	**0.16**	**0.16**	**0.17***	1.00
∞	0.00	0.00	0.00	0.00	0.00	0.00	0.00	0.00	0.00	0.00	0.00	$(1+2a/b)^{-1}$

In **bold** type are represented the 15 different nanostrengths measured on single-walled carbon nanotubes in bundle [5]; whereas in *italic* type we report the 19 nanostrengths measured on multiwalled carbon nanotubes [6], and in underlined type the most recent 18 observations [8]. All the data are reported with the exception of the five smallest values of 0.08, 0.10 [8], 0.11 [6], 0.12 [6,8] and 0.13 [5], for which we would need for example adjacent vacancies ($2b/q \sim 1$) in number $n = 2a/q = 138$–176, 90–109, 75–89, 64–74 and 55–63, respectively. The 26 strengths measured in [7] are also treated (asterisks), simply assuming two interacting walls for $100 < \sigma_N^{(exp)} \leqslant 200$ GPa (thus $\sigma_N = \sigma_N^{(exp)}/2$) or 3 interacting walls for $200 < \sigma_N^{(exp)} \leqslant 300$ GPa ($\sigma_N = \sigma_N^{(exp)}/3$). All the experiments are referred to $\sigma_N^{(theo)} = 100$ GPa ($q \sim 0$ 25 nm). If all the nanotubes in the cable contain identical holes, $\sigma_C/\sigma_C^{(theo)} = \sigma_N/\sigma_N^{(theo)}$.

with $\sigma_0 \approx 108$ GPa (but not significant for the strength of a single nanotube) and $w \approx 1.8$ (coefficient of correlation 0.94). In Fig. 1, the new data set [8] is treated by applying NWS ($N_N \equiv 1$, $w \approx 2.2$, $\sigma_0 \approx 25$ GPa) and compared with the other nanoscale statistics [3,35] for the other data sets [5–7]. Note that volume- or surface-based Weibull statistics

Table 3
Defect sizes and shapes identification (a,b) and related flaw-tolerant taper ratios $\lambda(a,b)$ according to the present analysis applied to nanotensile tests [5–8]

λ	$2b/q$											
$2a/q$	0	1	2	3	4	5	6	7	8	9	10	∞
0	1.90*	1.90*	1.90*	1.90*	1.90*	1.90*	1.90*	1.90*	1.90*	1.90*	1.90*	1.90
1	2.48*	2.37	2.25	2.18	2.13	2.09*	2.07*	2.05	2.03	2.02	2.01	1.90
2	3.04	2.91*	2.73*	2.59	2.48*	2.40	2.33	2.28*	2.25	2.21	2.19	1.90
3	3.61	**3.48**	3.25*	3.04	2.87	2.74*	2.64*	2.56	2.49*	2.44	2.39	1.90
4	**4.20**	4.06	**3.79**	3.53*	3.30*	3.12	2.97	2.86	*2.76*	2.68	2.61	1.90
5	4.82	4.67	4.36*	4.04	**3.76**	3.53*	3.34*	3.18*	3.05	2.94	2.85	1.90
6	5.46	5.31	4.97	4.60	4.26*	3.97	3.73*	3.53*	3.36*	3.23*	3.11	1.90
7	*6.14*	5.98	***5.60***	*5.18*	4.78	***4.44***	**4.15**	3.90	3.70*	3.53*	3.39*	1.90
8	**6.86**	*6.68*	*6.28*	***5.80***	5.34	4.94	4.59	4.30*	4.06	**3.85**	3.68*	1.90
9	**7.61**	**7.43**	**6.99**	*6.46*	5.94	5.47	5.07	4.73	***4.44***	**4.20**	3.99	1.90
10	8.40*	8.21*	7.74	**7.16**	*6.57*	6.04	***5.58***	*5.19*	4.85	4.57	4.33*	1.90
11	**9.24**	**9.03**	8.53*	7.89	**7.25**	*6.65*	*6.12*	***5.67***	*5.29*	4.96	4.68	1.90
12	*10.12*	*9.90*	**9.36**	8.67*	7.96	**7.29**	*6.70*	*6.19*	***5.75***	5.38	5.06	1.90
13	11.04	10.81	*10.23*	**9.49**	8.71*	7.97	**7.31**	*6.74*	*6.24*	5.82	5.46	1.90
14	*12.01*	*11.77*	11.16	10.35	**9.50**	8.69*	7.96	**7.32**	*6.76*	*6.29*	5.88	1.90
15	**13.03**	**12.78**	*12.13*	11.26	10.34	**9.45**	8.65*	7.93	**7.31**	*6.78*	*6.32*	1.90
16	*14.10**	*13.84**	**13.15**	*12.22*	11.23	*10.26*	**9.37**	*8.58**	7.90	7.31	**6.80**	1.90
17	*15.23**	*14.95**	*14.22**	**13.23**	*12.16*	11.11	*10.14*	**9.27**	8.51*	7.86	**7.29**	1.90
18	**16.41**	**16.11**	*15.34**	*14.29**	**13.14**	*12.00*	10.94	*9.99*	**9.16**	8.44*	7.82	1.90
19	**17.65***	**17.33***	**16.52**	**15.41**	*14.17**	**12.94**	*11.79*	10.76	*9.85*	**9.06**	8.37*	1.90
20	**18.94***	**18.62***	**17.76***	**16.57**	*15.25**	*13.93**	**12.69**	*11.57*	10.57	*9.71*	**8.96**	1.90
21	*20.30*	*19.96*	**19.05***	**17.80***	**16.39**	*14.97**	**13.63**	**12.41**	*11.33*	10.39	*9.57*	1.90
22	*21.72*	*21.36*	*20.41*	**19.08***	**17.58***	**16.06**	*14.62**	**13.31**	*12.14*	11.11	*10.22*	1.90
23	*23.21*	*22.83*	*21.83*	*20.43*	**18.84***	**17.21**	**15.66**	*14.24**	**12.98**	*11.87*	10.90	1.90
24	*24.76*	*24.37*	*23.32*	*21.84*	*20.15*	**18.42***	**16.76**	*15.23**	*13.86**	**12.66**	*11.61*	1.90
25	*26.39*	*25.98*	*24.88*	*23.32*	*21.52*	**19.68***	**17.90***	**16.26**	*14.79**	**13.49**	*12.36*	1.90
26	*28.08*	*27.66*	*26.50*	*24.86*	*22.96*	*21.00*	**19.10***	**17.35***	**15.77**	*14.37**	**13.14**	1.90
27	*29.86*	*29.41*	*28.20*	*26.47*	*24.47*	*22.38*	*20.36*	**18.49***	**16.79**	*15.29**	*13.97**	1.90
28	*31.71*	*31.24*	*29.97*	*28.16*	*26.04*	*23.83*	*21.68*	**19.68***	**17.87***	**16.25**	*14.83**	1.90
29	*33.64*	*33.15*	*31.83*	*29.92*	*27.68*	*25.35*	*23.06*	20.93	**18.99***	**17.26**	**15.74**	1.90
30	*35.65*	*35.14*	*33.76*	*31.75*	*29.40*	*26.93*	*24.51*	22.24	*20.17*	**18.32***	**16.68**	1.90
31	*37.75*	*37.22*	*35.77*	*33.67*	*31.20*	*28.59*	*26.02*	23.60	*21.40*	**19.42***	**17.68***	1.90
32	**39.93***	**39.38***	*37.87*	*35.67*	*33.07*	*30.32*	*27.60*	25.03	*22.69*	*20.58*	**18.71***	1.90
33	**42.21***	**41.63***	**40.06***	*37.75*	*35.02*	*32.12*	*29.25*	26.53	*24.03*	*21.79*	*19.80*	1.90
34	**44.58***	**43.98***	**42.34***	**39.92***	*37.06*	*34.00*	*30.97*	28.09	*25.44*	*23.05*	*20.93*	1.90
35	**47.05***	**46.42***	**44.71***	**42.19***	**39.18***	*35.97*	*32.76*	29.72	*26.91*	*24.37*	*22.12*	1.90
36	**49.61**	**48.97**	**47.18***	**44.54***	**41.39***	*38.01*	*34.64*	31.42	*28.44*	*25.75*	*23.36*	1.90
37	**52.28**	**51.61**	**49.75**	**46.99***	**43.69***	**40.14***	*36.59*	33.19	*30.04*	*27.19*	*24.65*	1.90
38	**55.06**	**54.36**	**52.42**	**49.54**	**46.09***	**42.36***	*38.62*	35.04	*31.71*	*28.69*	*25.99*	1.90
39	**57.94**	**57.21**	**55.19**	**52.20**	**48.58***	**44.68***	**40.74***	36.97	*33.45*	*30.26*	*27.40*	1.90
40	**60.94**	**60.18**	**58.08**	**54.96**	**51.18**	**47.08***	**42.95***	38.97	*35.27*	*31.89*	*28.86*	1.90
41	**64.05**	**63.27**	**61.08**	**57.82**	**53.87**	**49.59**	**45.25***	**41.06***	*37.16*	*33.59*	*30.39*	1.90
42	**67.28**	**66.47**	**64.19**	**60.80**	**56.68**	**52.19**	**47.64***	**43.24***	*39.12*	*35.36*	*31.98*	1.90
43	**70.64**	**69.79**	**67.43**	**63.89**	**59.59**	**54.90**	**50.13**	**45.51***	**41.17***	*37.21*	*33.64*	1.90
44	**74.12**	**73.24**	**70.79**	**67.11**	**62.62**	**57.71**	**52.72**	**47.86***	**43.31***	*39.13*	*35.36*	1.90
45	**77.73**	**76.82**	**74.27**	**70.44**	**65.76**	**60.64**	**55.41**	**50.31**	**45.52***	**41.13***	*37.16*	1.90
46	**81.48**	**80.53**	**77.88**	**73.90**	**69.03**	**63.68**	**58.20**	**52.86**	**47.83***	**43.21***	*39.03*	1.90
47	85.36	84.38	**81.63**	**77.49**	**72.41**	**66.83**	**61.10**	**55.51**	**50.23**	**45.37***	**40.97***	1.90
48	89.39	88.37	85.52	**81.22**	**75.93**	**70.10**	**64.12**	**58.26**	**52.72**	**47.61***	**42.99***	1.90
49	93.56	92.51	89.55	85.08	**79.57**	**73.50**	**67.25**	**61.12**	**55.31**	**49.95**	**45.09***	1.90
50	97.88	96.79	93.72	89.08	**83.35**	**77.02**	**70.50**	**64.08**	**58.00**	**52.38**	**47.27***	1.90
∞	∞	∞	∞	∞	∞	∞	∞	∞	∞	∞	∞	$1.9^{(1+2a/b)}$

In **bold** type are treated the 15 different tensile tests on single-walled carbon nanotubes in bundle [5], in *italic* type the 19 tests on multiwalled carbon nanotubes [6], whereas in underlined type the 18 new observations [8]. All the data are reported with the exception of the five smallest values of 0.08, 0.10, 0.11, 0.12 and 0.13 for which we would need related flaw-tolerant taper ratios of 3051, 613, 342, 210, and 139 respectively. The 26 strengths measured in [7] are also treated (asterisks), simply assuming two interacting walls for $100 < \sigma_N^{(exp)} \leqslant 200$ GPa (thus $\sigma_N = \sigma_N^{(exp)}/2$) or 3 interacting walls for $200 < \sigma_N^{(exp)} \leqslant 300$ GPa ($\sigma_N = \sigma_N^{(exp)}/3$). All the experiments are referred to $\sigma_N^{(theo)} = 100$ GPa ($q \sim 0.25$ nm).

Table 4
The new results [8] are here treated with respect to both strength and elasticity, assuming the presence of transversal nanocracks composed by n adjacent vacancies

MWCNT number and fracture typology	Strength (GPa)	Young's modulus (GPa)	κ	n	v (%)
1 (Multiple load A)	8	1100	1.01	148	0.07
2 (Clamp failed)	10	840	0.98	100	0.23
3	12	680	1.00	69	0.44
4 (Failure at the clamp)	12	730	0.98	69	0.40
5 (Multiple load B)	14	1150	1.02	51	0.14
6 (Multiple load a)	14	650	0.97	51	0.62
7	15	1200	1.05	44	0.11
8	16	1200	1.02	39	0.13
9	17	960	1.00	34	0.49
10	19	890	0.97	27	0.74
11 (Multiple load b)	21	620	0.99	22	1.51
12 (Multiple load I)	21	1200	0.99	22	0.22
13 (Multiple load II)	23	1250	0.99	18	0.17
14	30	870	1.00	11	1.92
15 (Plasticity observed)	31	1200	0.59 (0.99)	10	0.49
16 (Plasticity observed)	34	680	0.69 (1.02)	8	3.80
17 (Multiple load III)	41	1230	1.03	5	0.69
18 (Failure at the clamp)	66	1100	0.98	2	4.90

The constitutive parameter κ has been estimated as $\kappa \approx \ln(\varepsilon_N)/\ln(\sigma_N/E)$ for all the tests: note the low values for the two nanotubes that revealed plasticity (in brackets the values calculated up to the incipient plastic flow are also reported). The ideal strength is assumed to be of 100 GPa and the theoretical Young's modulus of 1300 GPa; the crack length n is calculated from Eq. (2) and introduced in Eq. (8) to derive the related vacancy fraction v ($\xi = \pi/2$). Fracture in two cases was observed at the clamp; in one case the clamp itself failed, thus the deduced strength represents a lower bound of the nanotube strength. Three nanotubes were multiple loaded (in two a, b and A, B or in three I, II, III steps), i.e., after the breaking in two pieces of a nanotube, one of the two pieces was again tested and fractured at a higher stress. Two nanotubes displayed a plastic flow. A vacancy fraction of the order of few parts per thousand is estimated, suggesting that such nanotubes are much more defective than as imposed by the thermodynamic equilibrium (see Section 2), even if the defects are small and isolated. However, note that other interpretations are still possible, e.g., assuming the nanotube is coated by an oxide layer and rationalizing the ratio between the observed Young's modulus and its theoretical value as the volumetric fraction (for softer coating layers) of carbon in the composite structure.

are identical in treating the external wall of the tested nanotubes, just an atomic layer thick. We have also found a poor coefficient of correlation treating this new data set with classical Weibull statistics, namely 0.51 (against 0.88 for NWS, see Fig. 1).

All these experimental data [5–8] are treated in Table 2, by applying QFM in the form of Eq. (2): nonlinear multiple solutions for identifying the defects corresponding to the measured strength clearly emerge; however, these are quantifiable, showing that a small defect is sufficient to rationalize the majority of the observed large strength reductions. In Table 3 the related taper ratios corresponding to flaw-tolerant megacables are reported, according to Eq. (3): taper ratios of about two order of magnitudes higher than the theoretical value are suggested by our analysis, in contrast to the current proposal [9,10], for which the cable failure is thus predicted.

Finally, the new experimental results [8] are differently treated in Table 4, with respect to both strength and elasticity, assuming the presence of transversal nanocracks. The ideal strength is assumed to be 100 GPa and the theoretical Young's modulus 1 TPa; the crack length n is calculated from Eq. (2) and introduced in Eq. (8) to derive the related vacancy fraction v ($\xi = \pi/2$).

9. Size effects

For a megacable, classical Weibull statistics [36] is more appropriate. For such a case, $N_N = V/V_0$, and the characteristic volume V_0 is here assumed, for consistency with NWS [35], as the volume of a single nanotube (V is the volume of the megacable): thus N_N represents the number of nanotubes contained in the megacable. Accordingly, a size effect in the (over-)simplified form of a power law, i.e., $\sigma_N = \sigma_0 N_N^{-1/w}$ is predicted for the nominal failure stress: as it is well known, larger is weaker. As discussed in Section 4, LEFM would yield $w = 6$. Note that Weibull statistics is also successfully applied to the fatigue strength (or lifetime), which is therefore expected to be reduced in larger structures.

Researchers [37] have recently been able to build the first meter-long cable based on carbon nanotubes. For such a nanostructured macroscopic cable, a strength–density ratio of $\sigma_C/\rho_C \approx 120$–$144$ kPa/(kg m^{-3}) (or for a densified cable $\sigma_C/\rho_C \approx 465$ kPa/(kg m^{-3})) was measured, dividing the breaking tensile force by the mass per unit length of the cable, since the cross-sectional geometry was not clearly identified. The cable density was estimated to be $\rho_C \approx 1.5$ kg m^{-3}, resulting in a cable strength of $\sigma_C \approx 200$ kg m^{-3}. Thus, we estimate for the single nanotube contained in such a cable $\sigma_N \approx 170$ MPa (carbon density 1300 kg m^{-3}), much lower than its theoretical or measured nanoscale strength, in agreement with our discussion. Assuming the nanotubes investigated at the nanoscale [5–8] to be one micron long and the cable [37] one meter in length, we can roughly estimate $w \approx -\ln(1/10^{-6})/\ln(31/0.17) \approx 2.7$ (or $w \approx 3.3$ for a densified cable; see Ref. [3] for details). Noting that the megacable volume is of the

order of $10^8 \times 10^{-1} \times 10^{-6} = 10\,\mathrm{m}^3$ and a nanotube has a volume of the order of $10^{-8} \times 10^{-8} \times 10^{-6} = 10^{-22}\,\mathrm{m}^3$, it follows that $N_N \approx 10^{23}$ nanotubes are expected, corresponding (according to the previous power-law scaling) to a negligible megacable strength. However, a deviation from a power-law is expected [25] according to the pioneer paper by Carpinteri, suggesting the following nano/mega scaling [38] as a function of the surface–volume ratio A/V of the cable:

$$\frac{\sigma_C(A/V)}{\sigma_N} = \left(\frac{(\sigma_N/\sigma_M)^{1/\alpha} - 1}{\tilde{q}A/V + 1} + 1 \right)^{-\alpha} \tag{10}$$

in which σ_N denotes the strength of the single nanotube, i.e., the nanoscale strength ($\tilde{q}A/V \to \infty$), σ_M the megascale strength ($\tilde{q}A/V \to 0$) and $\sigma_C(A/V)$ the strength of a cable with a given size and shape. The reader can here consider this equation as an asymptotic matching between the nanoscale and the megascale strength, with a transition dictated by the characteristic material length $\tilde{q}$ (related to its microstructure or fracture quantum; see Ref. [38] for details); α is the maximum value of the power of the singularity. Note that for the classical case of $\alpha = 1/2$ (LEFM), for self-similar cables (V/A is proportional to the cable length L) and for $\sigma_N/\sigma_M \to \infty$, as in usual material applications, Eq. (12) becomes identical to the well-known Carpinteri scaling law [25], that can thus be considered having a "universal" nature (see our commentary [39]). Note that the maximum slope $\alpha = 1$ (in a log–log plot) would represent a limit, in our context for hyperelastic materials with $\kappa \to \infty$ (see Section 4), in agreement with previous and independent discussions [40,41].

For the megacable, imposing $\sigma_N \approx 100$ GPa, we have a preliminary estimate from in-silicon experiments using the SE^3 code of $\sigma_M \approx 15$ GPa [3]; thus, again, a large strength reduction is expected at the megascale, if compared with the nanoscale strength. This is not surprising: in the megacable cross-section $\sim 10^9$ filaments will be present, and since at the thermal equilibrium $n \approx 10^{12-20}$, each of them will contain $\sim 10^{3-11}$ vacancies, sufficient to strongly reduce the megacable strength. Thus, even if the theoretical nanotube strength could be observed in nanoscale experiments, as perhaps for the WS_2 nanotubes experimentally [7,42] and theoretically [14] investigated, large strength reductions are unavoidable at the megascale. Multiscale simulations of a stretched defective megacable composed by millions of billions nanotubes are in progress with the SE^3 code.

10. Conclusions

The strength of a real, thus defective, carbon nanotube based space elevator megacable is expected to be reduced by a factor of at least $\sim$70% [3] with respect to the theoretical strength of a carbon nanotube, in contrast to claims of the current design [9,10]. Further studies on the role of defects are required. Accordingly, in this paper key simple formulas for the design of a flaw-tolerant space elevator megacable have been reported, suggesting that it would need a taper ratio (for uniform stress) of about two orders of magnitude larger than that currently proposed. A strength reduction by a factor of $\sim$70% would correspond to a taper ratio of $\sim$8.5, perhaps still achievable, but expected to be strongly larger for a slightly larger strength reduction, e.g., $\sim$613 for a strength reduced to 1/10 of its theoretical value (as strength reduction observed also at the nanoscale).

Several new results have been reported in this paper. In particular, in Section 2 we have demonstrated and quantified the vacancy fraction at the thermodynamic equilibrium. In Section 3 the first self-consistent law for the strength reduction of a single nanotube or of a nanotube bundle containing defects with given size and shape is derived; the taper ratio for a flaw-tolerant space elevator cable is accordingly obtained. In Section 4 elastic plasticity (or hyperelasticity), rough cracks and finite domains are discussed, extending the law presented in Section 2. In Section 5 the fatigue lifetime is evaluated for a single nanotube and for a nanotube bundle. In Section 6 the related Young's modulus degradations due to the presence of defects are quantified. In Sections 7 and 8 the new results on strength and elasticity are compared with all the main atomistic simulations and tensile tests on carbon nanotubes presented in the literature. Finally, in Section 9, size effects are discussed. We suggest that size effects are statistically unavoidable and are expected to play a fundamental negative role in so huge a cable. Thus, the design of the space elevator cable requires much more caution: a megacable is not simply a giant defect-free nanotube.

Acknowledgements

The author acknowledges the support of the Italian Ministry of University and Research (MIUR) and thanks A. Carpinteri for discussion and Dorothy Hesson for the final English grammar supervision.

References

[1] Artsutanov YV. Kosmos na Elektrovoze, Komsomol-skaya Pravda, July 31 (1960); contents described in Lvov, V. Science 1967;158:946–7.
[2] Pearson J. The orbital tower: a spacecraft launcher using the Earth's rotational energy. Acta Astronaut 1975;2:785–99.
[3] Pugno N. On the strength of the nanotube-based space elevator cable: from nanomechanics to megamechanics. J Phys–Condens Mat 2006;18:S1971–90.
[4] Iijima S. Helical microtubules of graphitic carbon. Nature 1991;354:56–8.
[5] Yu MF, Files BS, Arepalli S, Ruoff R. Tensile loading of ropes of single wall carbon nanotubes and their mechanical properties. Phys Rev Lett 2000;84:5552–5.
[6] Yu MF, Lourie O, Dyer MJ, Moloni K, Kelly TF, Ruoff R. Strength and breaking mechanism of multiwalled carbon nanotubes under tensile load. Science 2000;287:637–40.
[7] Barber AH, Kaplan-Ashiri I, Cohen SR, Tenne R, Wagner HD. Stochastic strength of nanotubes: an appraisal of available data. Compos Sci Technol 2005;65:2380–6.

[8] Ding W, Calabri L, Kohlhaas KM, Chen X, Dikin DA, Ruoff RS. Modulus, fracture strength, and britlle vs plastic response of the outer shell of arc-grown multiwalled carbon nanotubes. Exp Mech 2006;47:25–36.
[9] Edwards BC. Design and deployment of a space elevator. Acta Astronaut 2000;10:735–44.
[10] Edwards BC, Westling EA. The space elevator: a revolutionary earth-to-space transportation system. Spageo Inc; 2003.
[11] Pugno N. A quantized Griffith's criterion, fracture nanomechanics, meeting of the Italian group of fracture. Italy: Vigevano; 2002. September 25–26.
[12] Pugno N, Ruoff R. Quantized fracture mechanics. Philos Mag 2004;84:2829–45.
[13] Pugno N. Dynamic quantized fracture mechanics. Int J Fracture 2006;140:158–68.
[14] Pugno N. New quantized failure criteria: application to nanotubes and nanowires. Int J Fracture 2006;141:311–28.
[15] Kittel C. Introduction to solid state physics. New York: John Wiley; 1966.
[16] Bhadeshia HKDH. 52nd Hatfield memorial lecture – large chunks of very strong steel. Mater Sci Technol 2005;21:1293–302.
[17] Fan Y, Goldsmith BR, Collins PG. Identifying and counting point defects in carbon nanotubes. Nat Mater 2005;4:906–11.
[18] Ippolito M, Mattoni A, Colombo L, Pugno N. The role of lattice discreteness on brittle fracture: how to reconcile atomistic simulations to continuum mechanics. Phys Rev B 2006;73:104111-1–6.
[19] Taylor D, Cornetti P, Pugno N. The fracture mechanics of finite crack extensions. Eng Fract Mech 2005;72:1021–8.
[20] Pugno N, Ciavarella M, Cornetti P, Carpinteri A. A unified law for fatigue crack growth. J Mech Phys Solids 2006;54:1333–49.
[21] Pugno N, Cornetti P, Carpinteri A. New unified laws in fatigue: from the Wöhler's to the Paris' regime. Eng Fract Mech 2007;74:595–601.
[22] Rice JR, Rosengren GF. Plane strain deformation near a crack tip in a power-law hardening material. J Mech Phys Solids 1968;16:1–12.
[23] Carpinteri A, Pugno N. Fracture instability and limit strength condition in structures with re-entrant corners. Eng Fract Mech 2005;72:1254–67.
[24] Carpinteri A, Chiaia B. Crack-resistance behavior as a consequence of self-similar fracture topologies. Int J Fracture 1996;76:327–40.
[25] Carpinteri A. Scaling laws and renormalization groups for strength and toughness of disordered materials. Int J Solid Struct 1994;31:291–302.
[26] Wang QZ. Simple formulae for the stress-concentration factor for two- and three-dimensional holes in finite domains. J Strain Anal 2002;73:259–64.
[27] Pugno N. Young's modulus reduction of defective nanotubes. Appl Phys Lett 2007;90:043106.
[28] Pugno N, Troger H, Steindl A, Schwarzbart M. On the stability of the track of the space elevator. In: Proceedings of the 57th international astronautical congress. Spain: Valencia; 2007. October 2–6.
[29] Mielke SL, Troya D, Zhang S, Li J-L, Xiao S, Car R, et al. The role of vacancy defects and holes in the fracture of carbon nanotubes. Chem Phys Lett 2004;390:413–20.
[30] Belytschko T, Xiao SP, Ruoff R. Effects of defects on the strength of nanotubes: experimental–computational comparisons, Los Alamos National Laboratory, Preprint Archive, Physics, arXiv:physics/0205090; 2002.
[31] Zhang S, Mielke SL, Khare R, Troya D, Ruoff RS, Schatz GC, et al. Mechanics of defects in carbon nanotubes: atomistic and multiscale simulations. Phys Rev B 2005;71:115403-1–115403-12.
[32] Khare R, Mielke SL, Paci JT, Zhang S, Ballarini R, Schatz GC, et al. Coupled quantum mechanical/molecular mechanical modelling of the fracture of defective carbon nanotubes and grapheme sheets. Phys Rev B 2007;75:075412.
[33] Meo M, Rossi M. Tensile failure prediction of single wall carbon nanotube. Eng Fract Mech 2006;73:2589–99.
[34] Sammalkorpi M, Krasheninnikov A, Kuronen A, Nordlund K, Kaski K. Mechanical properties of carbon nanotubes with vacancies and related defects. Phys Rev B 2004;70:245416-1–8.
[35] Pugno N, Ruoff R. Nanoscale Weibull statistics. J Appl Phys 2006;99:1–4.
[36] Weibull W. A statistical theory of the strength of materials, 151. Handlingar: Ingeniörsvetenskapsakademiens; 1939.
[37] Zhang M, Fang S, Zakhidov AA, Lee SB, Aliev AE, Williams CD, et al. Strong, transparent, multifunctional, carbon nanotube sheets. Science 2005;309:1215–9.
[38] Pugno N. A general shape/size-effect law for nanoindentation. Acta Mater 2007;55:1947–53.
[39] Carpinteri A, Pugno N. Are the scaling laws on strength of solids related to mechanics or to geometry? Nat Mater 2005;4:421–3.
[40] Carpinteri A, Pugno N. Scale-effects on average and standard deviation of the mechanical properties of condensed matter: an energy-based unified approach. Int J Fracture 2004;128:253–61.
[41] Carpinteri A, Chiaia B, Cornetti P. A scale-invariant cohesive crack model for quasi-brittle materials. Eng Fract Mech 2002;69:207–17.
[42] Kaplan-Ashiri I, Cohen SR, Gartsman K, Ivanovskaya V, Heine T, Seifert G, et al. On the mechanical behavior of WS_2 nanotubes under axial tension and compression. Proceedings of the national academy of science USA 2006;103:523–8.